Air entrainment by a viscous jet plunging into a bath

Élise Lorenceau and David Quéré
Physique de la Matière Condensée, UMR 7125 du CNRS, Collège de France, France

Jens Eggers
School of Mathematics, University of Bristol, University Walk, Bristol BS8 1TW, United Kingdom

(Dated: October 8, 2004)

A liquid jet plunging into a container of liquid often entrains a thin film of air with it, producing bubbles. This bubble production is detrimental to many industrial processes, such as filling a container with a molten glass or polymer, or in coating processes. Conversely, in making a foam one uses this effect, hence it is important to control the rate of bubble production. Here, we measure the amount of air entrained by a viscous jet over a wide range of parameters and explain the phenomenon theoretically. A simple scaling argument accurately predicts entrainment rates over 4 orders of magnitude in the dimensionless jet speed.

PACS numbers: 47.15.Rq, 47.15.Gf, 47.55.Dz

Air entrainment is a common phenomenon that can be encountered in many environmental situations - as in breaking waves or steep chutes which contributes to river oxygenation- or in various industrial processes - such as aeration of water in open channels, coating processes or pouring of liquids. A paradigm for air entrainment is a jet plunging into a bath of fluid. If the fluid viscosity is small (e.g. water) [1–3], air entrainment only occurs if it is provoked by perturbing the jet. If the viscosity is higher (100 times that of water or more) [4, 5], air entrainment occurs *spontaneously*, by producing an air film. Here we present the first experimental measurements of entrainment rates and explain the results theoretically.

As described in [4–8], the liquid/air interface is hollowed by the flow of the plunging jet and a dip is formed around the fluid stream. Such a profile, which is continuous as long as the velocity V of the jet is constant, can be seen in Fig. 1 a). Something more dramatic happens if V increases above a threshold value V_c. The stationary profile ceases to exist and a film of air is entrained with the jet into the bath. This gaseous film, which wraps around the liquid jet, decays into air bubbles a few centimeters below the surface [9]. This phenomenon is of tremendous practical importance: in many industrial processes a viscous liquid (typically molten glass, metal or polymer) is poured inside a mold and the formation of bubbles damages the quality of the molded object.

Previous studies have focused on the threshold velocity V_c below which no air is entrained. At speeds close to V_c the interface at the bottom of the hollow region is very close to a cusp (see the circled zone of Fig.1 a)). Such singular features of free surfaces were first reported by Joseph et al. [10], and analyzed theoretically by Jeong and Moffatt [11], who found that a local balance between viscosity η and surface tension γ produces curvatures which increase exponentially with the capillary number $Ca = \eta V/\gamma$.

Any increase in jet velocity leads to a large decrease of the radius of curvature at the tip of the cusp. As pointed out in [6], this eventually results in the destruction of this tip: the upper fluid (usually air, of viscosity η_0), is forced into the tip and back out again by the external flow, and thus exerts a lubrication pressure on it. Below a critical tip radius (thus above a critical jet velocity), the tip "cracks" and a thin film of the upper fluid (often air) is entrained inside the bath [4], [12], [13]. In [6] it was shown that this critical tip radius increases with η_0/η, which together with Moffatt's law for the critical radius yields a threshold velocity $V_c \propto \ln(\eta/\eta_0)$, as was recently confirmed experimentally [7, 8].

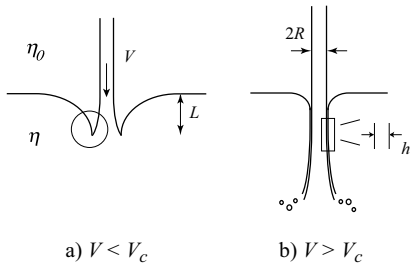

FIG. 1: Experimental set-up. A cylindrical liquid jet of viscosity η, surrounded by a fluid medium of viscosity η_0 plunges into a bath of the same liquid. The diameter of the jet is of order of 5 mm. On the left the velocity of the jet is below the threshold velocity, on the right it is above, hence the jet entrains an air film of thickness h into the bath.

Just below V_c, we experimentally find the depth L of the region hollowed by the jet (cf. Fig.2 (a)) to be about 1 cm, several times the capillary length. This agrees with the estimate of $L \approx \sqrt{\eta V_c/\rho g}$, which follows from balancing viscous forces with gravity [7]. The surface deformation as measured by L thus far exceeds the capillary length $\kappa^{-1} = \sqrt{\gamma/\rho g}$, which results from a capillary - gravity balance.

The temporal development of the air film displayed in Fig.2 indeed illustrates these different features. A jet 5 mm in diameter (about 1000 times more viscous than wa-

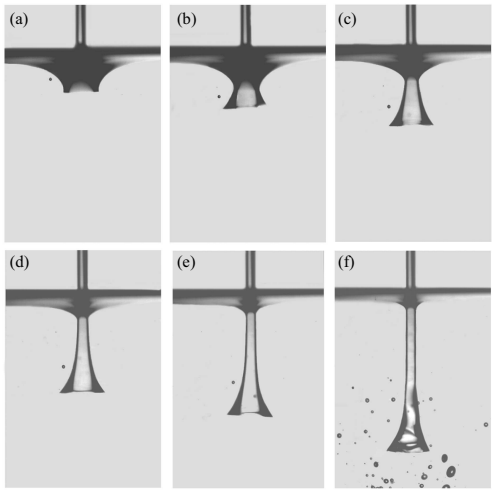

FIG. 2: A jet of viscous liquid (here silicone oil of viscosity $\eta = 970$ mPa.s) and diameter 5mm impinging on a bath of the same liquid. Below a threshold velocity, the jet hollows the bath surface to a depth L, which increases with jet velocity up to a value of about 1cm (a). Above this threshold, air is entrained with the jet ((b) to (e)), and forms a stationary trumpet-like shape (f). At the same time, the surface of the bath around the jet relaxes to the shape of a static non-wetting meniscus, whose size is in the order of millimeters. The interval between two successive pictures is 130 ms. Note that the black line at the edge of the jet is no indication of the film thickness; it is due to the reflection of light by the curved air film of lower index of refraction.

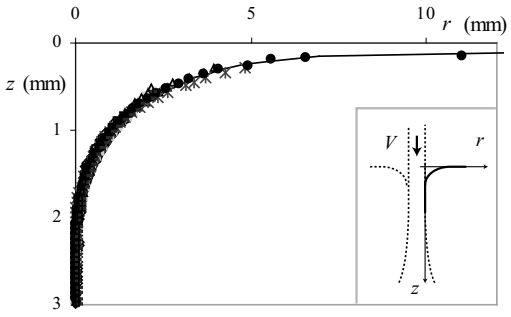

FIG. 3: Profile of the interface between the bath and the film of air, deduced from photographs such as Fig.2 (f), shown as the black line in the inset. The depth of the meniscus is plotted as a function of the radial position, and only the upper half of the trumpet shape is shown, where the profile is still vertical. The different data points correspond to different jet velocities (all above the threshold velocity of air entrainment), between 0.7 and 2.2 m/s. All the data collapse onto the full line, the static profile of a non-wetting meniscus.

ter) plunges into a bath of the same liquid. The jet velocity is controlled by the height of the reservoir from which the jet is formed. It is measured with a fast camera by following the motion of particles inserted randomly into the jet. Right above the interface, the velocity profile was observed to be a plug flow. In Fig.2(a), the jet velocity is below the velocity of entrainment ($V < V_c$), hence the profile observed is stationary. The height of the reservoir and therefore the velocity of the jet is slightly increased between panel (a) and (b). This rise has a dramatic effect: the interface breaks and the jet entrains with it a thin air film (looking black because of light reflection). Its length grows from panel (b) to (f) where it reaches its final stationary trumpet shape. This shape is expected since the jet slows down as it enters the bath, and conservation of mass implies a gradual increase in radius (from which we can deduce the jet velocity as it penetrates the bath). At a certain depth (of several centimeters), the film decays into bubbles which are then driven upward, and burst when they reach the surface. Note the velocity of the jet remains constant from panels (b) to (f).

The formation of the new stationary state (panel f) is accompanied by a considerable reduction in surface deformation of the bath. This is because the air film now "lubricates" the entry of the fluid jet, and shear stresses both inside the jet and in the liquid bath are greatly reduced. Instead, the shape of the bath surface close to the jet is now set by a purely *static* balance of gravity and surface tension forces, as confirmed by our measurements of the interface shape presented in Fig.3. We superimpose profiles of the final shape (cf. Fig.2 (f)) corresponding to different jet velocities, and compare them to the shape of a static meniscus (full line). The latter is obtained by integrating the Laplace equation $\gamma C = \rho g z$ (C is the interface curvature) twice, assuming a "contact angle" of 180° with the air film, and a flat profile for $z = 0$. The remarkable consequence of this observation is that for $\eta \gg \eta_0$ the fluid viscosity η becomes inconsequential, and the rate of air entrainment is determined by the speed of the jet and the viscosity of the entrained fluid η_0 alone.

Accordingly, we measured the variation of the film thickness h with jet speed for different values of η_0. In the case of oil films (between 10 and 30 times the viscosity of water) in a glycerol bath the film thickness could be measured optically. To measure the thickness of the film of air (a few microns), we determined the total volume of the air bubbles being formed, thus giving the flow rate of air. Knowing the mean velocity of the air film - i.e. half the velocity of the jet - and the radius of the jet R, we can deduce the thickness of the film. Note that we measure R close to the surface, where it is very nearly constant, indicating that the jet speed is also constant and equal to the original jet velocity.

We find that for a given liquid-liquid or gas-liquid system, the film thickness increases with the jet velocity like a power law V^α, best fits giving $\alpha = 0.7 \pm 0.1$ (cf. Fig.4). In fact, using a simple scaling argument based on our previous observations, we are able to quantitatively describe *all* our data. Namely, the film is sustained by the interplay between surface tension forces in the outer meniscus (which oppose the film's formation) and the vis-

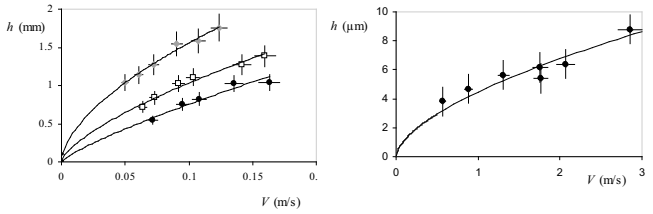

FIG. 4: Thickness of the film entrained by a glycerol jet ($\eta = 900$ mPa.s) impacting a bath of glycerol. (a.) Oil films (the black, white and gray symbols designate silicone oils of respective viscosity $\eta_0 = 8, 20$ and 32 mPa.s). (b.) Air film ($\eta_0 = 2 \cdot 10^{-2}$ mPa.s). Note the difference in thickness between both cases. The fits are scaling laws of the form V^α , giving in both cases $\alpha = 0.7 \pm 0.1$

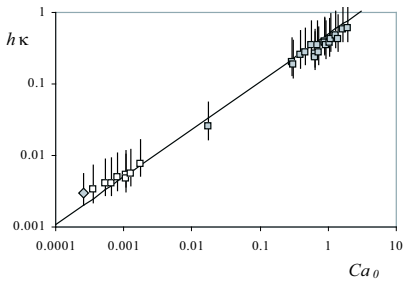

FIG. 5: Thickness of the entrained film (empty symbols: air; full ones: silicone oils) normalized by the capillary length, as a function of the capillary number $Ca_0 = \eta_0 V/\gamma$, for a glycerol jet in a glycerol bath (except for the diamond, which is obtained using a silicone oil of same viscosity yet different surface tension as glycerol). Because of the large interval explored here, both scales are logarithmic. The data are fitted by a straight line corresponding to equation (1), with prefactor 0.5 ± 0.2.

cous forces inside the thin film (which are responsible for entrainment). Equating pressure *gradients* at the junction between the static meniscus and the film, we obtain

$$\kappa\gamma/\lambda \approx \eta_0 V/h^2.$$

On the right appears the classical expression for the lubrication pressure gradient [18] based on the film's viscosity η_0, on the left the gradient of curvature. To estimate the latter, we introduced a typical length scale λ over which the film thickness is varying in the matching region. To determine λ we observe that the curvature of the film and of the static meniscus must match, yielding

$$\kappa \approx h/\lambda^2.$$

Combining both equations yields our central result

$$h \approx \kappa^{-1}(\eta_0 V/\gamma)^{2/3}. \quad (1)$$

The predictive power of this expression is best appreciated by summarizing our data for different upper viscosities η_0 in a *single* plot using the appropriate capillary number $Ca_0 = \eta_0 V/\gamma$. As shown in Fig.5, equation (1) correctly predicts the film thickness over 4 orders of magnitude in the capillary number, and for a variety of different fluid-fluid and air-fluid systems. The straight line of figure 5 represents equation (1), including a prefactor 0.5 ± 0.2 which has been fitted to the data.

It has not escaped our notice that the arguments leading to (1) are the same used to derive the well-known Landau-Levich law [14, 15] for the thickness of the *fluid* film entrained on a *solid* plate or fiber being withdrawn from a bath of viscous liquid [16]. In that case, the prefactor of equation (1) has been calculated and found equal to 0.9. Quite surprisingly, very similar arguments still apply in our case, but with the liquid jet assuming the role of the solid plate, and the air the role of the viscous fluid. The reason is that the air film serves to isolate the jet from the rest of the fluid, such that the viscous fluid no longer plays a dynamical role, but just supplies the boundary conditions.

In fact the boundary conditions that apply here are slightly different from those of the classical Landau-Levich problem. Namely, the outer boundary condition for the film now is that of a deformable solid, which changes the prefactors, but not the scaling laws. Schwartz et al. showed that a solid-like boundary thickens the entrained film (by a factor of $2^{2/3}$)[17], which physically is due to the increased resistance of the capillary back-flow, making it less efficient than in the presence of a free boundary. Combining the prefactor of 0.9 given by the classical Landau-Levich law and the correction cited above give a prefactor of 1.4 for equation (1), which is three times larger than the one we found experimentally.

The change in boundary condition toward that of a solid also affects the flux of entrained matter: since the flow in the entrained film has a Couette profile, (instead of being a plug flow, as in a classical Landau-Levich film), we find $Q = 2\pi RhV/2$ for the flux, denoting the jet radius as R. Thus the flow of air depends strongly (like $V^{5/3}$) on the velocity, as suggested by everyday experience: we all know that the injection of air into an egg white is considerably enhanced by using a (fast) beater rather than a fork.

Fig.5 shows that (1) still describes our data for capillary numbers approaching unity, which can be understood by an argument proposed by Derjaguin [18]. For Ca_0 larger than unity, the meniscus is no longer quasi-static, but deformed by the flow, and gravity (instead of surface tension) becomes the force opposing entrainment. Balancing gravity $\Delta\rho g$ with the viscous force $\eta_0 V/h^2$ immediately yields $h \sim \kappa^{-1}(\eta_0 V/\gamma)^{1/2}$ as the entrainment law at large capillary number. This slight difference in exponent (1/2 instead of 2/3) implies a gradual transition toward another scaling law for large Ca_0, with relatively small corrections to (1) for $Ca_0 < 1$.

However, we do note that the high capillary number

data fall below the line given by (1), which is probably the result of the transition toward the new power law. Fitting the prefactor only to the low capillary number data would increase it and bring it closer to the theoretical prediction. To fully understand the origin of the remaining discrepancy in the prefactor, a full asymptotic analysis taking into account the antagonist curvature of the jet (which tends to thin the jet) would be needed, but it is beyond the scope of this letter.

Our results might be relevant to both the making of foams, as well as for the understanding of the way emulsions form. The main remaining obstacle is to elucidate the role of surfactants in both processes, which is the next step in our research program. We also expect that the rate of air entrained by solids plunging into a viscous bath - which has never been explained to the best of our knowledge - should be given by the same arguments, the air film similarly allowing a decoupling between the moving solid and the quiescent bath.

Note finally that a similar phenomenology is observed in a variety of situations where entrainment is forced externally, for example by a rotating cylinder [10]. Another example consists in extracting the upper liquid from a two-fluid interface through a pipette (selective withdrawal) [19]. Above a threshold velocity, a very thin stream of the lower liquid is extracted as well. However in these cases there is no decoupling between the extracted liquid and the quiescent bath, so our reasoning does not apply. Instead, an alternative scaling theory was recently put forward for selective withdrawal [20].

In conclusion we have presented a unifying picture for the rate of air entrainment into a viscous fluid, both by impacting jets and solids. The rate depends strongly on the jet velocity, while the fluid viscosity is unimportant. A number of related entrainment phenomena remain to be understood.

We thank Frédéric Restagno, Frédéric Chevy and Etienne Reyssat for very valuable discussions and suggestions.

[1] Y. Zhu, H. N. Ogũz, and A. Prosperetti, J. Fluid Mech. **401**, 151 (2000).
[2] C. D. Ohl, H. N. Ogũz, and A. Prosperetti, Phys. Fluids **12**, 1710 (2000).
[3] B. Kersten, C.D. Ohl, and A. Prosperetti, Phys. Fluids **15**, 821 (2003).
[4] T. Lin and H. Donelly, A.I.Ch.E. J. **12**, 563 (1981).
[5] A.K. Bin, Chem. Eng. Sci. **15**, 367 (1993).
[6] J. Eggers, Phys. Rev. Lett. **86**, 4290 (2001).
[7] E. Lorenceau, F. Restagno, and D. Quéré, Phys. Rev. Lett. **90**, 184501 (2003).
[8] A. Cartellier and J. Lasheras, 3rd European-Japanese Two-Phase flow group meeting, (2003).
[9] C. Clanet and J. Lasheras, Phys. Fluids **9**, 1864 (1997).
[10] D. Joseph, J. Nelson, M. Renardy, and Y. Renardy, J. Fluid Mech. **223**, 383 (1991).
[11] J.-T. Jeong and H.K. Moffatt, J. Fluid Mech. **241**, 1 (1992).
[12] P.G. Simpkins and V. Kuck, Nature (London) **403**, 641 (2000).
[13] S. Thorrodsen and Y.-K. Tan, Phys. Fluids **16**, L13 (2004).
[14] L. Landau and V. Levich, Acta Physicochimica USSR **17**, 42 (1942).
[15] B. Derjaguin, Dokl. Acad. Sci. USSR **39**, 13 (1943).
[16] We have been informed by A. Cartellier that A. Linan has made the same observation, unpublished (2003).
[17] L. Schwartz, H. Princen, and A. Kiss, J. Fluid Mech. **172**, 259 (1986).
[18] B. Derjaguin and S. Levi, Film coating theory, London: The Focal Press(1964).
[19] I. Cohen and S. Nagel, Phys. Rev. Lett. **88**, 074501 (2002).
[20] W.W. Zhang, Phys. Rev. Lett. to be published, (2004).